

# Multi-Disciplinary Challenges in Tissue Modeling for Wireless Electromagnetic Powering: A Review

Kara N. Bocan, *Student Member, IEEE*, Marlin H. Mickle *Life Fellow, IEEE*, and Ervin Sejdić, *Senior Member, IEEE*

**Abstract**—Wireless electromagnetic powering of implantable medical devices is a diverse research area, with goals including replacing percutaneous wires, miniaturizing and extending the lifetime of implanted devices, enabling wireless communication and biosensing, all while maximizing safety and efficiency of wireless power transfer. Many challenges in wireless transcutaneous powering are associated with tissue as an electromagnetic transmission medium. Tissue is lossy and variable, and safety is a concern due to absorption of electromagnetic energy in high-water-content tissue. The purpose of this overview is to summarize reported variability of tissue properties, particularly in the context of electromagnetic safety, with a focus on models of tissue that can represent variability in the design and evaluation of systems for wireless transcutaneous power transfer.

**Index Terms**—wireless power transfer, implantable medical devices, tissue dielectric properties, transcutaneous energy transfer

## I. INTRODUCTION

PROPERTIES of the tissue environment provide significant challenges for wirelessly powering implantable medical devices. Although many technologies have been investigated for wireless implantable devices, including ultrasound and piezoelectric energy harvesters, electromagnetic power transfer has emerged as the method with greatest power delivery capability over a range of power requirements and implanted device dimensions and locations [1]. Further discussions of electromagnetic power transfer efficiency and comparisons to other powering methods are provided in [2]–[4]. Wireless electromagnetic powering of implantable devices requires power transfer through tissue, using external and implanted antennas to transmit and receive electromagnetic energy, forming a transcutaneous antenna system. Tissue properties are of practical interest in application to electromagnetic wireless powering due to their effects on antenna impedance, power transfer, and safety.

Tissue is a dielectric material, with electromagnetic behavior described by properties of conductivity, permittivity, and permeability [5]–[8]. Tissue is considered non-magnetic, therefore the properties of most interest are conductivity and permittivity. These values can be complex, and represent energy storage and loss in a material [9], [10]. Tissue electromagnetic properties are functions of molecular and atomic mechanisms such as molecular dipole polarization and movement of ions [6], [10]–[12]. In fact, it is impossible to distinguish between

real and imaginary components of complex permittivity or conductivity without molecular or atomic interpretation [12].

The efficiency of transcutaneous antenna systems is a function of tissue properties, as the efficiency of a system is a measure of power transfer and absorption in tissue [12], [13]. Safety is of particular concern in transcutaneous systems, because the absorption of electromagnetic energy in tissue can lead to tissue heating, causing patient discomfort and/or tissue damage [5], [14], [15]. Differences in both tissue geometry and tissue properties will affect electromagnetic energy transfer and absorption. Whether these effects are significant to the function of a system is heavily dependent on the application and the properties of the system.

Due to the effects of tissue properties on transcutaneous systems, and the associated safety concerns, it is of interest to develop test beds to evaluate the effects of electromagnetic devices on tissue, to address safety issues in the design phase. This includes simulations as well as physical tissue phantoms for experimental verification. Tissue absorption is difficult to measure with physical phantoms and tends to be evaluated in simulation, typically in terms of the specific absorption rate (SAR), which relates absorption to electric field distribution and tissue properties [16], [17]. Tissue phantoms can physically approximate tissue electromagnetic properties of conductivity and permittivity within a frequency range of interest, and are used in experimental evaluation of transcutaneous systems to corroborate simulations [16], [18]–[20].

There are many considerations involved in choosing appropriate tissue models for the design and evaluation of transcutaneous systems, including antenna topology, dimensions, separation, and electromagnetic operating frequency. The presence of tissue near an antenna affects antenna impedance and electrical size, as any dielectric and/or lossy medium affects the field distribution near an antenna [21]. Tissue proximity has been investigated for different antenna topologies, and reviews of antennas and electromagnetic frequencies for transcutaneous systems are provided in [1]–[3], [22]. However, there are few studies that investigate the effects of tissue *variability* on transcutaneous systems, using variable tissue models in simulation or experimental validation [23]. The focus of this work is therefore on reported variability of tissue properties, how variability affects electromagnetic safety, and how variability can be modeled during the design and evaluation of transcutaneous powering systems.

The paper is organized as follows: The first section reviews literature reports of tissue properties (conductivity and permittivity) and their variations; the next section relates tissue

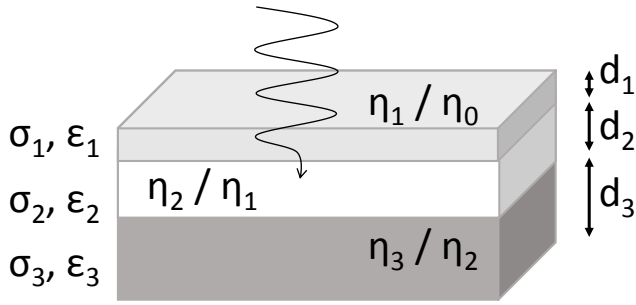


Fig. 1. Tissue parameters that affect electromagnetic behavior and are known to vary among people and over time: layer conductivity ( $\sigma$ ) and permittivity ( $\epsilon$ ), layer thicknesses ( $d$ ), and intrinsic impedance ratios at tissue interfaces ( $\eta$ ) as determined by relative properties of adjacent layers.

variability to electromagnetic safety, with a discussion of SAR and mechanisms of tissue heating; the last section reviews existing tissue models and tissue phantoms used for evaluating electromagnetic safety, with a focus on which phantoms could be used to represent variability in tissue properties. In each of these sections, we draw and consolidate information from various areas of literature including hyperthermia, bioimpedance, dosimetry, electromagnetic physics, antenna theory, and wireless power transfer.

## II. TISSUE PROPERTIES AND VARIATIONS

This section reviews measurements of tissue properties reported in the literature and discusses mechanisms of tissue property variations. It is well-established that tissue properties vary over frequency [6], but the focus of this background is on reports of tissue properties/parameters and how they vary among people and within a single person over time. A system is typically designed with a target operating frequency, but tissue properties are functions of tissue structure and composition as well as frequency. There is a spread in the values of tissue properties even at a single frequency, as noted in [6], and the goal of this section is to elucidate the causes of that spread. Figure 1 illustrates tissue properties that will be discussed in this work in terms of their variability and underlying causes of variability.

Dielectric properties of any material are prone to change with temperature, orientation, mixture, pressure, and molecular structure [10]. Tissue variations include changes in macroscopic tissue structure or body composition (tissue geometry, fat content, etc.), changes in water content and perfusion, and smaller-scale changes in ion or protein concentrations, cell size, and pH, among other mechanisms [11], [24]–[26].

### A. Measurements of Tissue Properties

Practical measurement issues must be considered when defining and comparing tissue properties. Although reported measurements of some tissues are available, there is a lack of *in vivo* measurements of human tissues due to obvious difficulties with measuring any but the most surface-level of tissues (such as the skin or tongue). Instead, tissue properties

are typically estimated from measurements of animal tissue, or measurements on excised human tissue with corrections for differences in temperature [6], [27].

The series of papers by Gabriel et al. [6]–[8] is widely cited as a reference for tissue properties in the electromagnetics literature, along with the associated database containing values of permittivity and conductivity of tissues at each frequency [28]. However, the values of permittivity and conductivity in the database represent values of the empirical model, fitted by Gabriel et al. to literature data and measurements [8]. The empirical model predicts values of permittivity and conductivity of each tissue at each frequency. However, additional consideration should be given to the variability in permittivity and conductivity at a given frequency, due to variability among tissue samples. For example, at a given frequency, the skin of one person is expected to have different values of conductivity and permittivity compared to another person, and it is possible that neither person’s skin matches the values predicted by the empirical model.

In their series of papers, Gabriel et al. [6] first presented a review of measured tissue properties in the literature, and then used those properties to fit their empirical model. As evidenced by the ranges of measured properties in the review, tissues that have been extensively studied (e.g., muscle) are likely more indicative of realistic variability among samples, because there are more representative data.

To ensure fair comparison, values must be compared with attention to the measurement method and tissue sample characteristics. Variations in reported properties can occur due to measurement uncertainty, differences in measurement methods, and sample preparation [6], [27], [29]. A common method of measuring tissue properties is the coaxial probe method, shown in Figure 2 using a dielectric probe kit (SPEAG DAK 3.5) and a vector network analyzer (Agilent 8753ES). Other common methods for measuring material properties are summarized in [10], but not all methods are practically applicable to tissue. Another method used in the literature involves a dielectric resonator in contact with the tissue [25]. These measurement methods utilize the input reflection coefficient to calculate dielectric properties of a material. Measurement uncertainty is higher for higher permittivity values, because there is less change in measured reflection coefficient for variations in material permittivity [10].

Tissue properties in the literature are often expressed in terms of impedance (or individually resistance, capacitance, or phase angle as components of impedance). Impedance is a function of dielectric properties as well as tissue geometry, and impedance measurements will be discussed where relevant.

### B. Tissue Variability and Mechanisms

There are obvious tissue variations among different body areas, including differences in tissue thicknesses, and the presence of different tissues at the abdomen compared to the head or the eye, for example [30], [31]. Differences in tissues are also expected among patients, such as differences in fat content and muscle mass [32]. Tissue structure differences are also relevant when using animal models. As mentioned

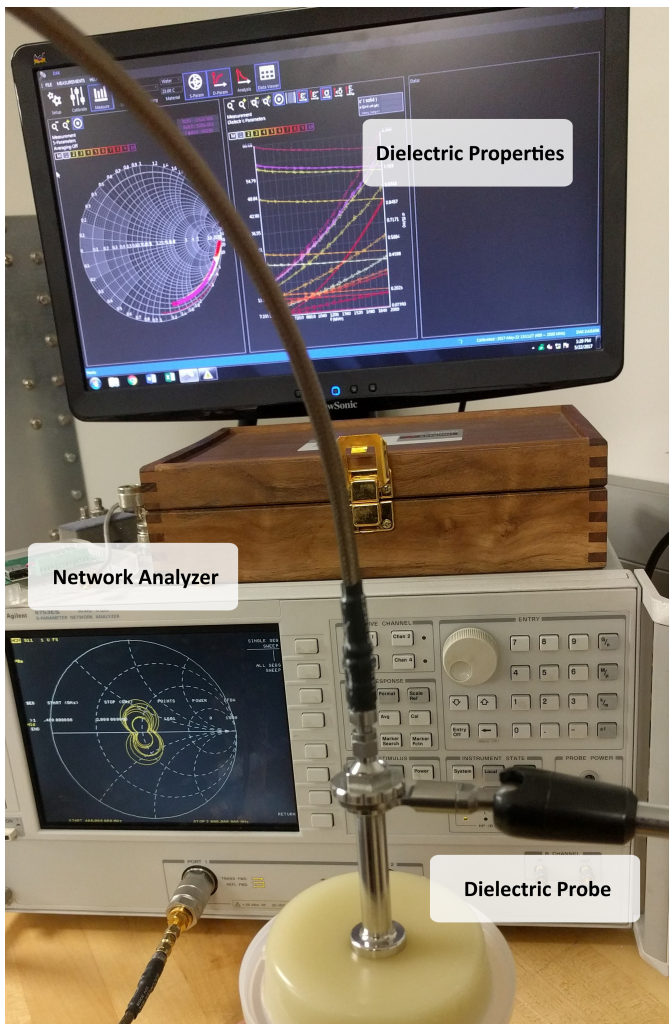


Fig. 2. Dielectric probe method for measuring material properties, using a dielectric probe (SPEAG DAK 3.5) and a vector network analyzer (Agilent 8753ES).

previously, due to the difficulty of measuring human tissues, tissue properties have been drawn from measurements of animal tissues, both *in vivo* and *ex vivo*. For example, the empirical model by Gabriel et al. [8] was built including measurements of animal tissue where *in vivo* human tissue measurements were scarce or not available.

Although differences in tissue thicknesses or shape would ideally not influence bulk tissue properties, tissue has an inhomogeneous cellular structure, and therefore changes in effective conductivity and permittivity may occur for different tissue geometries. This leads into a necessary discussion of the relationship between tissue structure and tissue dielectric properties (summarized in Figure 3).

Tissue can be classified into different types based on overall structure (e.g., skin, fat, muscle). The dielectric properties characterizing different tissue types are functions of this smaller-scale structure [33]. Schwan [34] classifies tissues into muscular or fat/bone tissue based on the ratio of water to protein content, with fat/bone tissue having a dielectric constant affected more strongly by small amounts of water and therefore being more variable from one sample to another.

Cellular variations contribute directly to tissue property variations. Tissue is inhomogeneous, and can only be approximated as homogeneous depending on the scale of interest (e.g., the electromagnetic operating frequency) [29]. As operating frequency increases, smaller tissue structures become more significant to tissue electromagnetic properties. Increased resistance and capacitance is associated with extracellular matrices and additional cells [32]. At a cellular level, muscle tissue is of particular interest due to its anisotropic structure; higher resistance is measured perpendicular to muscle fibers [32]. Jilani et al. [25] saw a minimal change in resonance frequency with muscle anisotropic variation, but greater dielectric sensitivity with measurements perpendicular to muscle fibers.

Studies of tissue water content have been extensively reported [24]–[26], [32], [35]–[39]. As evidenced by differences in water content among tissue types and differences in measured parameters reported in [6], [7], changes in tissue water content affect tissue dielectric properties. Although more hydration without a change in ion concentration decreases conductivity, tissues with greater body water content are more conductive, because body water comprises ions [8], [24], [25]. Changes in moisture levels lead to shifts in resonant frequency or quality factor, which are functions of conductivity and permittivity [36].

Total body water has been observed to decrease with age, attributed to changes in cell size, structure, water content, and free versus bound water [24], [27], [38], [39]. These mechanisms are exemplified during human brain development, where brain growth increases both the number of cells and their weight, and myelination during the first two years reduces overall ion concentration [24]. Due to age-related water loss, dielectric constant decreases at all frequencies and loss factor increases below 4 GHz [25]. The effect of changes in body water on tissue properties appears to be higher at higher frequencies [31], as Balidemaj et al. [27] did not see a significant change in conductivity at 128 MHz in their group of 20 subjects aged 30 to 86.

Bioimpedance measurements in combination with patient body measurements (e.g., height, weight) have been used to calculate estimates of parameters such as extracellular fluid volume or perfusion [26], [37]. Variations in impedance have been reported associated with tissue perfusion, where phase angle changes with blood volume [26]. Changes in membrane permeability affect intracellular fluid and extracellular fluid composition, and substance concentrations in intra- and extracellular fluids contribute to tissue properties, such as blood glucose and hematocrit [26], muscle pH [25], and protein and ion concentrations [11].

Tissue properties vary with temperature, which contributes to differences between properties measured *ex vivo* and *in vivo*. Balidemaj et al. [27] extrapolated conductivity measurements at room temperature to estimate conductivity at body temperature by adjusting values 2% per degree Celsius [35]. Hyperthermia studies have investigated tissue property changes with temperature *in vivo*, to address how changes in tissue properties will affect electromagnetic field distributions during hyperthermia treatments [17].

Pathological changes in tissue properties have also been

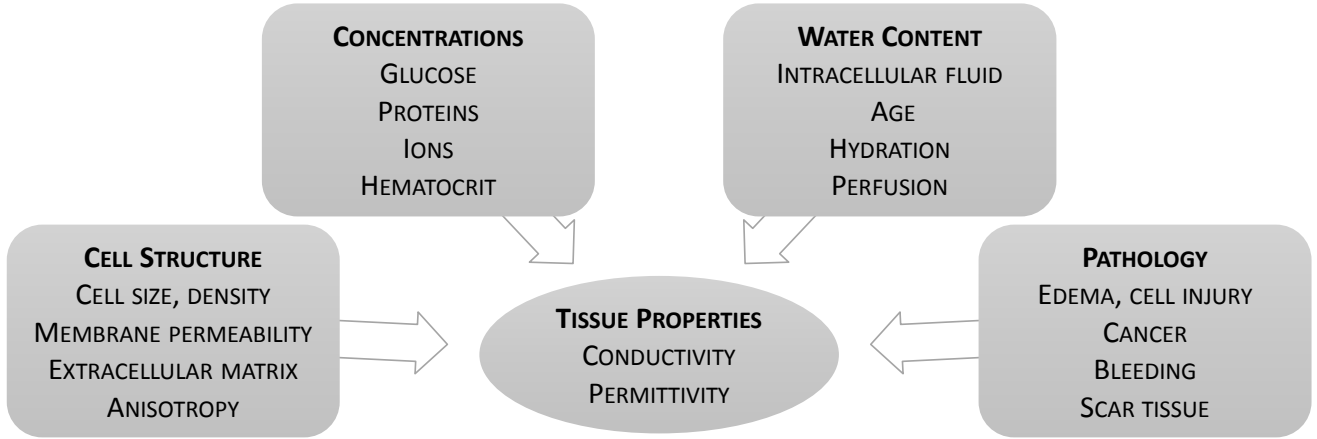


Fig. 3. Example factors that influence tissue electromagnetic behavior and determine properties of conductivity and permittivity.

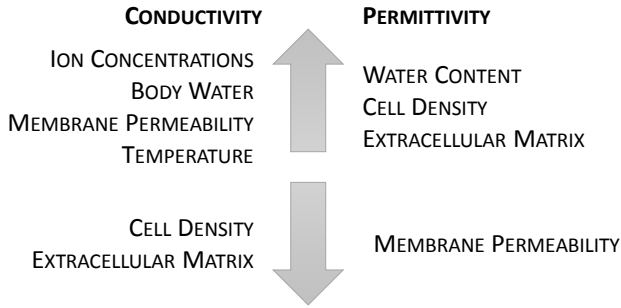


Fig. 4. Tissue parameters that have been related to increases or decreases in tissue dielectric properties of conductivity and permittivity.

studied, with the goal of diagnosing conditions based on measured changes in tissue properties. Cancerous tissues have been observed to have higher conductivity [27], [35], and higher permittivity [40], [41] compared to healthy tissue. Internal bleeding can be detected by measuring tissue properties [42]. Lower impedance is associated with edema or injury due to accumulation of extracellular fluid [26], [32]. Neuromuscular diseases are correlated with higher resistivity, and reductions in phase are correlated with disease progression [26]. Higher resistance and decreased reactance in muscle is associated with atrophy (due to smaller muscle) [32]. Increases in resistance are related to epithelial cell growth, and increased reactance is related to cell mass in wound healing [26]. Variable factors that have been associated with increases or decreases in conductivity and permittivity are summarized in Figure 4.

### III. TISSUE VARIATIONS AND ELECTROMAGNETIC SAFETY

The information in this section is drawn from multiple disciplines, including the literature on hyperthermia treatment, magnetic resonance imaging, and bioimpedance, where measurement of tissue parameters can indicate pathological

conditions (e.g., greater water content due to swelling). Information from these studies regarding relationships between absorption/heating and tissue parameters can then be applied to evaluating electromagnetic exposure and the safety of wireless transcutaneous systems.

This section begins with a discussion of electromagnetic absorption and tissue heating mechanisms and models, followed by a discussion of the effects of tissue variability on SAR and temperature rise.

#### A. Mechanisms of energy absorption and tissue heating

Absorption of electromagnetic energy in tissue can lead to tissue heating, and potentially tissue damage. Heating in wireless electromagnetic systems is most often evaluated in terms of SAR. SAR for a given point in a medium is defined according to IEEE Standard 1528-2013 [43] as in Equation 1, where  $E$  is electric field intensity,  $\rho$  is density, and  $\sigma$  is conductivity. The quantity can be integrated over a volume or mass of tissue, the specifics of which are defined by each SAR standard, as discussed below. SAR can also be estimated in terms of the temperature rise over a given exposure time for specified points in the tissue, as in Equation 2, where  $T$  is temperature,  $t$  is exposure time, and  $c$  is specific heat capacity.

$$SAR = \frac{\sigma |E|^2}{\rho} \quad (1)$$

$$SAR = c \frac{\Delta T}{\Delta t} \quad (2)$$

Several organizations have established SAR guidelines for electromagnetic exposure. Because SAR represents absorption of energy per unit mass, standards specify the mass over which to calculate average SAR, where X-g SAR denotes averaging over X g of tissue [16]. IEEE Standard C95.1 specifies peak 10-g SAR <2.0 W/kg and peak 1-g SAR <1.6 W/kg [44].

Current standards require a homogeneous tissue-equivalent liquid phantom to evaluate SAR. IEEE Standard 1528-2013 recommendations for SAR evaluation are with regard to exposures for wireless communications devices [43], and [45]



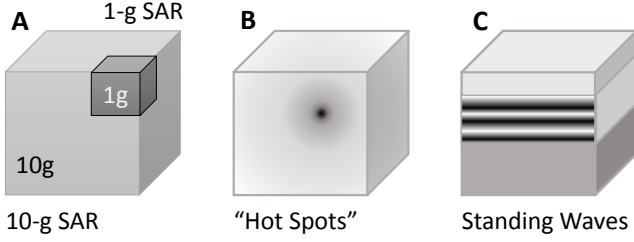


Fig. 5. Illustration of concepts relating to SAR calculations: (A) standard SAR averaging volumes, (B) “hot spots” or concentrated areas of absorption that contribute to high local SAR, and (C) reflections of electromagnetic energy at tissue interfaces that cause standing waves.

notes that SAR guidelines are specified in terms of far field parameters. Compared to far-field studies, there are relatively few studies on SAR and heat transfer due to near-field exposures [45].

It should be noted that SAR may not directly correspond to tissue heating [17], [46], because there can occur mm-sized “hot spots” that contribute to high local SAR, and potentially even smaller hot “nano spots” that are below the resolution of typical SAR calculations [47]. Reflections at tissue interfaces occur due to differences in intrinsic impedance ( $\eta = \sqrt{\mu/\epsilon}$ ) [9]. These reflections can cause heating due to standing waves within tissue layers, which can be a concern particularly at higher frequencies where tissue thicknesses are larger in proportion to the wavelength. For example, Schwan [34] suggested frequencies below 1 GHz to avoid standing waves in fat thicknesses up to 2.5 cm, to achieve targeted deep tissue heating under layers of subcutaneous fat. This is in the context of hyperthermia treatment, however the concept is applicable to a situation where there is a desired region of power delivery to an implanted antenna, but standing waves result in disproportionate field amplitudes and heating in surrounding tissue layers. Figure 5 summarizes concerns related to SAR calculations.

Thermal conduction can also contribute to tissue heating, for example through contact with the antenna, contact with implanted circuitry, or heat transfer from tissue to tissue [48]. This is not typically accounted for in SAR analyses. If waves penetrate to subcutaneous fat, the poor thermal conductivity between fat and the body surface leads to greater tissue heating [34].

Heat can be dissipated through the body’s thermoregulatory responses. Heat dissipation is less of a concern in electromagnetic systems because it counteracts temperature increases in tissue, and electromagnetic analyses are typically focused on “worst-case” tissue heating. However, thermoregulatory responses are still relevant to the present discussion on heating mechanisms. Heat loss is defined in terms of exposed body surface area - therefore depending on conditions including clothing, temperature, air movement, and humidity - and heat dissipation is more effective with shallower penetration of the electromagnetic waves (smaller skin depth) [5], [34]. Temperature increases will be greater in tissues with low blood flow; consequently, unpredictability of perfusion and other

thermal parameters means that SAR does not always correlate directly with temperature [17], [46].

Heat accumulation and loss in tissue have been described in equation form: the bioheat equation describes the temperature rise in tissue as a function of heat conduction, blood perfusion, and microwave heating [48]–[50]. Equation 3, used in [49], is based on the Pennes bioheat equation [50], where  $\rho$  is density,  $c$  is specific heat capacity,  $T$  is temperature,  $t$  is time,  $k$  is thermal conductivity,  $Q$  is metabolic heat generation rate,  $S$  is SAR,  $\omega$  is blood perfusion rate, and the subscript  $b$  denotes a blood property. The operator  $\nabla$  denotes the gradient (e.g.,  $\nabla x$ ) or divergence (e.g.,  $\nabla \cdot x$ ).

$$\rho c \frac{\partial T}{\partial t} = \nabla \cdot (k \nabla T) + \rho Q + \rho S - \rho_b c_b \rho \omega (T - T_b) \quad (3)$$

With reference to the heating mechanisms discussed above, it can be concluded that SAR estimated from a measured temperature rise over time (Equation 2) may actually underestimate the absorption of electromagnetic field energy, due to the body’s heat dissipation mechanisms *in vivo*, or due to heat loss through external surfaces of an *ex vivo* sample or phantom. Similarly, SAR estimated from measurements of the electric field (Equation 1) will depend on accuracy and homogeneity of a sample’s conductivity and density as well.

### B. SAR measurements

Wang et al. [16] provides a succinct description of SAR measurement techniques, which can be categorized into measurement of electric field or temperature increase. In the electric probe method, a robot arm moves an electric-field probe in a controlled pattern in a liquid phantom, to determine peak local and average SAR. In the thermographic method, a thermographic camera records temperature distribution in phantoms over a specified plane. This requires defining a split plane in the phantom, but is better than the electric-field probe method for measuring boundaries or solid phantoms [16]. Paulides et al. [17] used the electric probe method, scanning the 3D electric field distribution to verify simulations for hyperthermia treatments. IEEE Standard C95.3 attempts to standardize experimental SAR evaluation for human exposures [51]. The complexity of measuring electric field distributions and temperature leads most studies to estimate SAR through simulation [16], [17].

### C. Effects of property variations on SAR

Several studies have investigated body-scale structure variations and SAR, such as body part positions (effects of movement or distance from radiating antennas) [52], inclusion of surrounding body segments in simulation (effects of simplified simulation models) [43], [53], and fluid flow or perfusion [45]. The focus of this review is more on the effects of variability among patients and over time, including variations in dielectric properties.

The effects of dielectric property variations on SAR are not necessarily intuitive, and often complicated by other factors. Keshvari et al. [24] computed SAR with varying dielectric

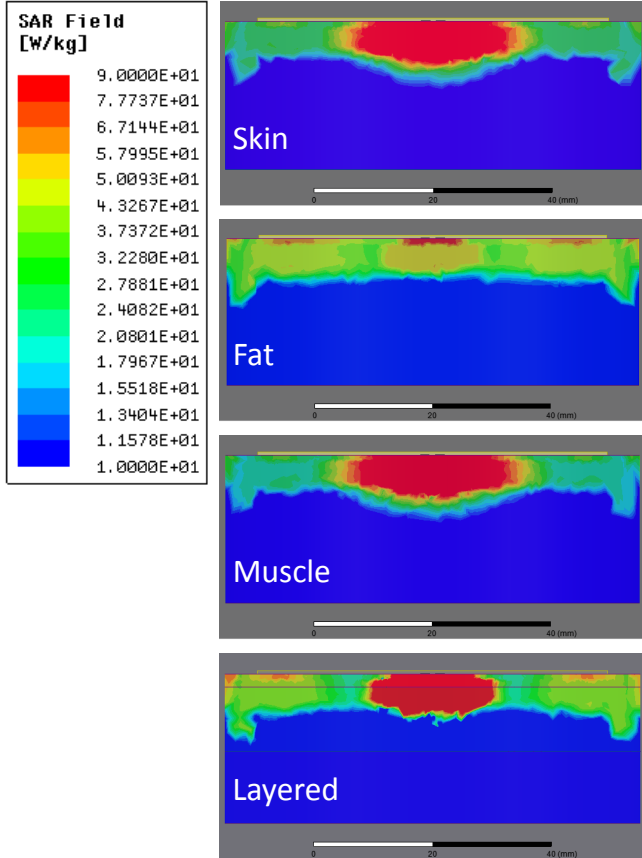


Fig. 6. Simulated 1-g SAR at 915 MHz near a 1 mm x 60 mm dipole antenna for tissue models with different conductivity ( $\sigma$ ), relative permittivity ( $\epsilon_r$ ), and structure: homogeneous models with properties of skin ( $\epsilon_r = 46.0$ ,  $\sigma = 0.850$ ), fat ( $\epsilon_r = 5.46$ ,  $\sigma = 0.0514$ ), or muscle ( $\epsilon_r = 55.0$ ,  $\sigma = 0.948$ ), and a layered model with skin (2.2 mm), fat (10.8 mm), and muscle.

parameters in detailed human models and a simplified muscle model, and observed that there was not always higher absorption in tissues with higher body water, and not always higher SAR with higher conductivity and permittivity. They concluded that “SAR variation depends not only on the increase in the dielectric values but also on ... anatomical shape of the models and the ratio of dielectric values in different tissue layers” [24]. Figure 6 shows an example of the different patterns of simulated 1-g SAR at 915 MHz (using ANSYS Electronics Desktop 2017.0) in tissue near a 1 mm x 60 mm dipole antenna, comparing homogeneous tissue models with properties of skin or muscle, and a layered model including skin, fat, and muscle, with dielectric properties from [8], [28].

In general, it has been shown that variations in tissue properties tend to affect maximum (local) SAR more than average SAR [29], [31], [52], [53]. Gajsek et al. [29] investigated effects of published dielectric parameter variability on local and whole-body SAR. They concluded that there is no universal approach to predicting relative changes in local SAR and effects of dielectric parameter variations should be validated for each case. Keshvari et al. [24] saw greater effects of SAR averaging volume at higher frequencies (>900 MHz). Dielectric property variations have less effect on SAR at higher

frequencies. Gajsek et al. [29] saw less change in local SAR with dielectric parameter changes at higher frequencies (2 GHz), and Keshvari et al. [24] observed that SAR variation with changes in dielectric values was smaller for 1.8 GHz and 2.45 GHz compared to 900 MHz.

SAR is more affected by changes in conductivity than permittivity [29], [54]. Gajsek et al. [29] saw significant variation in localized SAR when varying muscle parameters from 0.5 to 2.0 times the parameters reported by Gabriel et al. [7], with only minor changes seen when manipulating other tissue values such as fat, skin, or bone marrow. Monebhurrin et al. [54] found that maximum average simulated SAR is more sensitive to changes in conductivity than permittivity.

As stated earlier, SAR does not always directly correspond to tissue heating [17], [46]. There are relatively few studies of heat transfer specific to wireless transcutaneous systems (in comparison to studies of SAR), and even fewer on the effects of tissue property variations on tissue heating [45]. Most studies of tissue heating related to electromagnetic exposure are in the literature on hyperthermia treatment, where the goal is to selectively damage pathological tissues through targeted heating [17], [34]. Schwan [34] discussed effects of fat and skin thickness on heat absorption, concluding that absorption depends on fat thickness but that effects of skin thickness are relatively small due to skin electrical thickness below 3 GHz.

#### IV. ELECTROMAGNETIC MODELS OF TISSUE

Analytical, simulation, and experimental tissue models are essential for evaluating the safety of wireless transcutaneous systems in the design phase. This section reviews models used in the literature, focusing mainly on those used to evaluate wireless transcutaneous systems, but also drawing from literature on dosimetry or hyperthermia. The following is a brief review of existing models, with a discussion of which could be used to test effects of tissue variability in wireless transcutaneous systems.

In general, existing models are limited by imprecision in anatomy, tissue interfaces, and tissue properties [49]. Additionally, there are tradeoffs in modeling precision and simulation complexity, and difficulties constructing accurate experimental phantoms.

##### A. Analytical models

McAdams and Jossinet [55] provide a critical review of tissue circuit models, which is summarized here as its concepts are essential to evaluating electrical representations of tissue. Most circuit models include combinations of resistances and capacitances to represent the tissue medium, where the component values are functions of bulk tissue properties and tissue geometry.

In the Fricke model of tissue, shown in Figure 7A,  $R_1$  represents resistance of the suspending medium (extracellular fluid),  $R_2$  represents cell interiors (intracellular fluid), and  $C$  represents cell membrane capacitance [25], [55]. Intra- and extracellular fluids act as resistances due to their containing ions that conduct current and contribute to losses at higher frequencies. Cell membranes act as capacitors due to

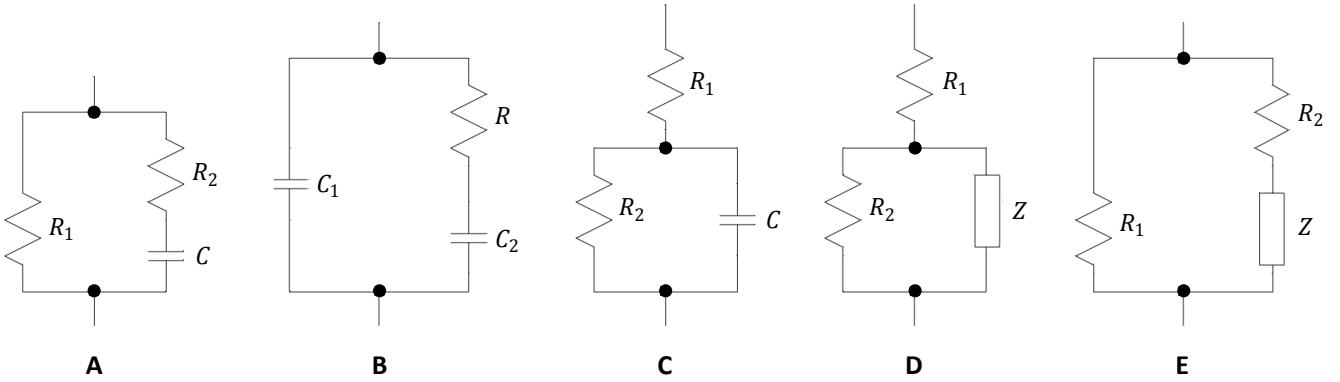


Fig. 7. Circuit models representing complex tissue impedance: Fricke (A), Debye (B), Lapicque (C), and Cole (D, E) [25], [55].

their structure as a dielectric material between two current-conducting electrolytes. Jilani et al. applied the Fricke model to evaluate tissue moisture content, fitting expressions of circuit components in the model using a ring resonator and measurements across a frequency range of 500 MHz - 20 GHz [25]. The ring resonator in their work is physically similar to antennas used for wireless powering. McAdams and Jossinet argue that the Fricke model best represents suspensions of red blood cells rather than other tissues, because it lacks an explanation for constant phase angle or the known frequency dependence of tissue resistance and capacitance [55].

The Debye model of tissue is based on molecular-level polarization mechanisms in tissue, and describes the dielectric behavior of a dilute suspension of free dipoles. The equivalent circuit model is a capacitor in series with a resistor both in parallel with a high frequency capacitor, as shown in Figure 7B [55]. The Debye model has been used to fit measured tissue data and predict tissue properties across frequency [35].

The Lapicque model (Figure 7C) includes similar components to the previously discussed models, with  $R_1$  representing intracellular fluid resistance, and  $R_2$  and  $C$  representing membrane resistance and capacitance, respectively [55]. More complex tissue circuit models have been developed building on the Lapicque model, including a constant-phase-angle frequency-dependent impedance,  $Z$  (Figure 7C and D) [55]. With appropriate definitions of the resistances and the impedance  $Z$ , these models become circuit representations of the Cole-Cole equation.

The Cole-Cole equation is an empirical model of tissue properties that provides a good fit to experimental data [8], [55]. Perhaps the most widely cited source of tissue properties, the aforementioned series of papers by Gabriel et al., fitted a Cole-Cole model to measurements of tissue properties over frequency [6]–[8]. However, [55] cautions against overreliance on the “relaxation” concept to relate the Cole-Cole function to the physics of tissue properties.

The Cole-Cole empirical model fitted by Gabriel et al. [8] has been widely used in the electromagnetic power transfer literature to determine permittivity and conductivity of various tissues at frequencies of interest, often in conjunction with simulated tissue models [13], [56]. Additionally, a web-

based tool has been developed to calculate model values for specified tissues and frequencies [28]. While expressions of tissue properties as functions of frequency are common, there is a comparative lack of expressions of tissue properties as functions of tissue parameters.

### B. Simulation models

Many simulation models of tissue have been constructed based on measurements and imaging of real tissue samples or body parts. Because tissue structure is heterogeneous, homogeneous models and phantoms have been used for reduced complexity [12], [54]. Depending on the frequency, homogeneous models may not accurately represent reflections at interfaces. This, in combination with uncertainty of dielectric properties, can lead to either under- or overestimating SAR, depending on the frequency [57]. Layered models are a step up in complexity from homogeneous models and include discrete layers of tissue types which are homogeneous within a layer, representing skin, fat, muscle, etc. The results of [24] support the use of layered models, especially at higher frequencies (>900 MHz) and when estimating SAR, because of how tissue composition affects field distribution and SAR hot spots [47].

More complex simulation models have been constructed based on imaging, such as CT scans or MRI. Data from the Visible Human project of the National Library of Medicine [58] was used in [29], [59], and other imaging-derived models include the Virtual Family [60], [61], and several detailed body part models [24], [31], [62]. This level of segmentation detail is most important for accurate prediction of hot spots and maximum SAR [17], [46]. There have been more recent efforts toward semi-automatic methods of importing and updating simulation model parameters from imaging data. Paulides et al. [17], [46] used a modified semi-automatic segmentation of tissues based on CT scans, using information from previous segmentations and combining with MRI scans. Dahdouh et al. [57] built upon such work with semi-automatic methods for transferring anatomy from a detailed model to a minimal model with simplified structure, using a Euclidean distance metric to compare positions of landmarks on models.

As simulation models become increasingly accurate, they also become increasingly specific to the anatomy used to

generate the model. Detailed models vary widely in dimensions [12], and abnormalities may be present in very accurate representative models [31]. Differences make comparisons difficult among studies, whether the differences are in overall geometry or limb positioning or smaller-scale structure [57].

The choice of dielectric properties is another source of variability among studies and potential inaccuracy to real operation. The choice of dielectric properties is complicated by limits on model complexity as well as uncertainty in reported dielectric property measurements. Homogeneous models typically use average dielectric parameters or parameters chosen to conservatively estimate absorption in heterogeneous tissue [31]. An effective dielectric constant can be used to represent multi-layered tissue, but it is highly dependent on tissue thicknesses and orientation [30], [42]. By this method, effective permittivity of a mixture of materials is skewed toward the material with higher permittivity [63]. Balidemaj et al. [27] note that some studies have used Cole-Cole model parameters from [8] for the bladder wall to represent the whole bladder, which does not sufficiently represent the higher conductivity of urine inside the bladder. Additionally, they indicate that measured conductivity of muscle was 14% higher than currently used in simulation models and measured bladder conductivity was an order of magnitude higher than used in many models [27]. Where human tissue properties are underreported, data from animal models are also common: Dahdouh et al. [57] used tissue properties interpolated from pigs, sheep, or rats in addition to measured properties of human tissues.

### C. Phantoms

Physical tissue models, or “phantoms”, are used for experimental validation of transcutaneous systems. In general, phantoms should represent the dielectric permittivity, conductivity and losses at the frequency of interest, in addition to preferably mimicking tissue structure and shape.

Some studies have used animal tissues (beef or pig skin, for example) to represent structural complexities of tissue. However, properties are unpredictable among samples and may vary from typical values of human tissues. Additionally, the properties of biological tissue are temperature- and time-dependent (particularly for excised tissue where the sample can dehydrate over time). An advantage of fabricated phantoms is the ability to design for properties at room temperature that mimic tissues at body temperature. A summary of excised tissue and phantom characteristics is provided in Table I.

This section discusses tissue phantoms that are designed to mimic human tissue properties *in vivo* (and the associated phantom “recipes”) in terms of ease of use, repeatability, and representation of tissue electromagnetic behavior.

1) *Gel phantoms*: Lazebnik et al. [18] reviewed gel phantom formulations along with their valid frequency ranges, and developed and characterized formulations of a wideband gel phantom with varying amounts of oil to adjust phantom properties. The phantom conductivity and permittivity were characterized for each amount of oil in the formulation, and the phantoms properties were shown to be stable up to nine weeks

TABLE I  
COMPARISON OF EXCISED TISSUE AND TISSUE PHANTOMS

Excised Tissue	Phantoms
+ Structural complexity	+ Repeatability
+ Representative properties	+ Controllable properties
– Sample variability	+ Stability
– Sample abnormalities	– Structurally simplistic
– Properties very sensitive to time, temperature	– Frequency limitations

TABLE II  
COMPARISON OF GEL AND LIQUID PHANTOMS

Gel	Liquid
+ Semi-solid structure	+ Simple fabrication
+ Layered phantoms	+ Easily variable properties
– More complex fabrication, cure time	– Containers, compartments for heterogeneous phantoms
– Adjusting properties can cause structural instability	– Frequency limitations

after fabricating. Porter et al. [19] used these formulations to build layered phantoms with properties mimicking skin, fat, and tumor tissues in the breast. Bakar et al. [20] adjusted the Lazebnik formulation to substitute formaldehyde. However, the fabrication of this phantom is somewhat complex, and the fat formulation shows less agreement with literature values [19]. Additionally, there may be concerns with the structural stability of the phantoms as the ratios of ingredients are changed.

Wang et al. [16] reviewed brain-equivalent and skull-equivalent agar phantoms. The brain-equivalent phantom comprised deionized water, agar, sodium chloride, sodium azide (as a preservative), TX-151 (for stickiness), and polyethylene powder. The skull-equivalent phantom comprised silicone emulsion, agar, glycerol (solvent), TX-151, and polyethylene powder. Polyethylene powder controls permittivity, while the salt controls conductivity, and the correct proportions of ingredients in each phantom depend on frequency.

IEEE Standard C95.3 references several formulations for muscle and other high-water-content tissues and other gel phantoms of varying viscosity, utilizing polyethylene powder to adjust permittivity and saline concentration to set conductivity [51], [64]–[66].

2) *Liquid phantoms*: Liquid phantoms represent tissue as homogeneous. Merli [12] used homogeneous liquid phantoms with muscle-like dielectric properties. Kibret et al. [67] used a vinyl cylinder filled with saline to represent the body at low frequency (<100 MHz). Wang et al. [16] reviewed an averaged tissue equivalent phantom for the body, composed of sugar, sodium chloride, deionized water, hydroxyethyl cellulose, bactericide, diethylene glycol butyl ether, Triton X-100, diacetin, and 1,2-propanediol. The SAM phantom, defined in IEEE Standard 1528-2013 [43] and used in [68], is an anthropomorphic-shaped phantom made of a low-permittivity,



TABLE III  
SUMMARY OF REPORTS AND ANALYSES OF VARIABILITY IN TISSUE ELECTROMAGNETIC PROPERTIES

Source	Tissue	Frequencies	Models/Methods
[6]–[8]	30 tissues (multiple species)	10 Hz - 20 GHz	measured properties, Cole-Cole
[53]	eye, head (12 tissues)	6 - 30 GHz	Debye, FDTD
[37]	skin	5 - 748 kHz	measured properties, Cole
[41]	breast (6 tissues)	488 kHz - 1 MHz	measured properties, Cole, Fricke
[38]	10 tissues (rat)	130 MHz - 10 GHz	measured properties, Cole-Cole
[29]	body (39 tissues)	70 MHz - 2.06 GHz	FDTD
[54]	head (10 tissues and homogeneous)	900, 1800 MHz	Visible Human, FDTD
[59]	body	400, 900, 2400 MHz	Visible Human, FDTD
[60]	body (51 tissues)	30 MHz - 3 GHz	FDTD
[24]	eye, head (15 tissues)	900, 1800, 2450 MHz	FDTD
[39]	head (16 tissues, porcine properties)	50 MHz - 20 GHz	measured properties, FDTD
[31]	eye, head (14 tissues)	0.9 - 5.8 GHz	FDTD
[25], [36]	muscle (chicken)	500 MHz - 20 GHz	Fricke, FEA
[52]	eye (6 tissues)	0.9 - 10 GHz	FDTD
[62]	skin (stratum corneum, epidermis, dermis, sweat ducts)	0.8 - 1.2 THz	FEA
[27]	muscle, bladder, cervix	128 MHz	measured properties, Cole-Cole
[57]	body (14 tissues)	2.1, 2.6 GHz	FDTD
[42]	head	0.75 - 2.55 GHz	FEA, phantom

low-loss plastic or fiberglass shell, filled with homogeneous tissue-equivalent liquid. Most of the rationale for the SAM phantom geometry and dimensions is based on wireless handset literature, and dimensions are selected from an anthropometric database of 1774 US Army males.

Homogeneous phantom properties must be chosen based on the heterogeneous tissue that they are representing, and are typically chosen to give a conservative estimate of absorption compared to real tissue. However, depending on the frequency, homogeneous phantoms may not accurately model standing waves within heterogeneous tissue, which can lead to greater heating. Table II summarizes general characteristics of both gel and liquid phantoms.

3) *Comments on phantoms:* Phantom dimensions are an important consideration in addition to phantom structure and properties [9]. IEEE Standard 1528 addresses advantages of anthropomorphic phantoms over flat or spherical phantoms for representing antenna loading/impedance and energy coupling into the phantom.

In general, phantoms are advantageous in that they can be used to test a physical system and corroborate simulation results. However, compared to simulation models, it is relatively difficult to fabricate phantoms that are complex and precise to the desired anatomy. The need for structural complexity has motivated the use of excised tissue in experimental validation, although this strategy presents its own problems, including unpredictability, aging and temperature effects, as mentioned

previously.

As noted in [43], a “90th-percentile head”, one possessing all of the 90th-percentile dimensions, does not exist. This supports the need for phantoms representing tissue variability that can be used in evaluating transcutaneous systems. A very precise phantom may be less important than a phantom that can be used to test the behavior of a system over a range of material properties. This is particularly relevant with recent research on adaptive transcutaneous systems [1].

## V. CONCLUSIONS AND FUTURE WORK

Tissue variability and modeling is an ongoing challenge in evaluating systems for wireless transcutaneous powering. The complexity of tissue structure makes predicting tissue properties difficult, as explored in bioimpedance studies and evidenced by ranges of reported tissue properties in the literature. As such, variation in properties must be considered when evaluating electromagnetic safety of wireless powering. Simulation models are increasingly precise and sophisticated, but can be limited by computational resources and specificity to an individual, as well as segmentation into tissue types and the choice of dielectric properties. Experimental validation depends on the use of excised tissue or fabrication of physical phantoms, which are limited by inaccuracies to human tissue properties *in vivo* and difficulties representing precise geometries, respectively. It is important to consider representation of tissue variability in the design and evaluation of systems for

transcutaneous powering, and to either compensate (adapt) or design for robustness to variations. A summary of studies of tissue variability is presented in Table III.

The future of the field of wireless transcutaneous powering will continue to be heavily cross-disciplinary, combining research on the biological side (bioimpedance, hyperthermia, electromagnetic dosimetry) with electromagnetics (dielectric materials, antenna theory, wireless power transfer). As reviewed in this work, background in each of these areas is necessary for design and evaluation of systems for wireless transcutaneous powering.

Future research efforts are most needed in the areas of quantifying variability among tissues, and developing both simulation and experimental models that can represent expected variability of tissue for designing and evaluating wireless powering systems. In simulation, this requires sensitivity analyses of the effects of variability in tissue structure and properties on system performance metrics such as power gain and SAR. Such analyses should be followed by experimental validation with variable phantoms, where heterogeneous phantoms are necessary to represent behavior at higher frequencies. In cases where a system cannot be designed to be insensitive to the effects of tissue variations, adaptive methods should be investigated.

## REFERENCES

- [1] K. N. Bocan and E. Sejdíć, "Adaptive transcutaneous power transfer to implantable devices: A state of the art review," *Sensors*, vol. 16, no. 3, 2016.
- [2] J. S. Ho, K. Sanghoek, and A. S. Y. Poon, "Midfield wireless powering for implantable systems," *Proceedings of the IEEE*, vol. 101, no. 6, pp. 1369–1378, 2013.
- [3] D. C. Ng, S. Bai, J. Yang, N. Tran, and E. Skafidas, "Wireless technologies for closed-loop retinal prostheses," *Journal of neural engineering*, vol. 6, no. 6, p. 065004, 2009.
- [4] A. B. Amar, A. B. Kouki, and H. Cao, "Power approaches for implantable medical devices," *Sensors (Basel)*, vol. 15, no. 11, pp. 28 889–914, 2015.
- [5] H. P. Schwan and G. M. Piersol, "The absorption of electromagnetic energy in body tissues; a review and critical analysis," *American Journal of Physical Medicine and Rehabilitation*, vol. 34, no. 3, pp. 425–448, 1954.
- [6] C. Gabriel, S. Gabriel, and E. Corthout, "The dielectric properties of biological tissues: I. Literature survey," *Physics in Medicine and Biology*, vol. 41, no. 11, pp. 2231–2249, 1996.
- [7] S. Gabriel, R. W. Lau, and C. Gabriel, "The dielectric properties of biological tissues: II. Measurements in the frequency range 10 Hz to 20 GHz," *Physics in Medicine and Biology*, vol. 41, no. 11, pp. 2251–2269, 1996.
- [8] —, "The dielectric properties of biological tissues: III. Parametric models for the dielectric spectrum of tissues," *Physics in Medicine and Biology*, vol. 41, no. 11, pp. 2271–2293, 1996.
- [9] C. A. Balanis, *Advanced engineering electromagnetics*. John Wiley & Sons, 2012.
- [10] *Basics of Measuring the Dielectric Properties of Materials*, Application Note 5989-2589, Agilent.
- [11] H. F. Cook, "The dielectric behaviour of some types of human tissues at microwave frequencies," *British Journal of Applied Physics*, vol. 2, no. 10, pp. 295–300, 1951.
- [12] F. Merli, "Implantable antennas for biomedical applications," Thesis, Ecole Polytechnique Federale de Lausanne, 2011.
- [13] A. S. Y. Poon, S. O'Driscoll, and T. H. Meng, "Optimal frequency for wireless power transmission into dispersive tissue," *IEEE Transactions on Antennas and Propagation*, vol. 58, no. 5, pp. 1739–1750, 2010.
- [14] A. W. Guy, J. C. Lin, P. O. Kramar, and A. F. Emery, "Effect of 2450-MHz radiation on the rabbit eye," *IEEE Transactions on Microwave Theory and Techniques*, vol. 23, no. 6, pp. 492–498, 1975.
- [15] A. Hirata, M. Fujimoto, T. Asano, W. Jianqing, O. Fujiwara, and T. Shiozawa, "Correlation between maximum temperature increase and peak SAR with different average schemes and masses," *IEEE Transactions on Electromagnetic Compatibility*, vol. 48, no. 3, pp. 569–578, 2006.
- [16] J. C. Wang, E. G. Lim, M. Leach, Z. Wang, and K. L. Man, "Review of SAR measurement methods in relation to wearable devices," *Engineering Letters*, vol. 24, no. 3, 2016.
- [17] M. M. Paulides, G. M. Verduijn, and N. Van Holthe, "Status quo and directions in deep head and neck hyperthermia," *Radiation Oncology*, vol. 11, no. 1, pp. 1–14, 2016.
- [18] M. Lazebnik, E. L. Madsen, G. R. Frank, and S. C. Hagness, "Tissue-mimicking phantom materials for narrowband and ultrawideband microwave applications," *Physics in Medicine and Biology*, vol. 50, no. 18, pp. 4245–4258, 2005.
- [19] E. Porter, J. Fakhoury, R. Oprisor, M. Coates, and M. Popovic, "Improved tissue phantoms for experimental validation of microwave breast cancer detection," *Proceedings of the Fourth European Conference on Antennas and Propagation*, 2010.
- [20] A. A. Bakar, A. R. Razali, N. A. Fauzi, and M. A. Murad, *Ultra Wideband Fat Tissue Fabrication Using Different Cross Linking Agent for Microwave Imaging*. Cham: Springer International Publishing, 2015, pp. 515–521.
- [21] C. A. Balanis, *Antenna Theory: Analysis and Design*. Hoboken, NJ: John Wiley and Sons, 2005.
- [22] A. Kiourti and K. S. Nikita, "A review of implantable patch antennas for biomedical telemetry: Challenges and solutions," *IEEE Antennas and Propagation Magazine*, vol. 54, no. 3, pp. 210–228, 2012.
- [23] K. N. Bocan, M. H. Mickle, and E. Sejdic, "Tissue variability and antennas for power transfer to wireless implantable medical devices," *IEEE Journal of Translational Engineering in Health and Medicine*, vol. In press, 2017.
- [24] J. Keshvari, R. Keshvari, and S. Lang, "The effect of increase in dielectric values on specific absorption rate (SAR) in eye and head tissues following 900, 1800 and 2450 MHz radio frequency (RF) exposure," *Physics in Medicine and Biology*, vol. 51, no. 6, p. 1463, 2006.
- [25] M. T. Jilani, W. P. Wen, L. Y. Cheong, and M. Z. ur Rehman, "A microwave ring-resonator sensor for non-invasive assessment of meat aging," *Sensors (Basel)*, vol. 16, no. 1, 2016.
- [26] H. C. Lukaski, "Evolution of bioimpedance: a circuitous journey from estimation of physiological function to assessment of body composition and a return to clinical research," *European Journal of Clinical Nutrition*, vol. 67, no. S1, pp. S2–S9, 2013.
- [27] E. Balidemaj, P. de Boer, A. L. H. M. W. van Lier, R. F. Remis, L. J. A. Stalpers, G. H. Westerveld, A. J. Nederveen, C. A. T. van den Berg, and J. Crezee, "In vivo electric conductivity of cervical cancer patients based on  $B_1^+$  maps at 3T MRI," *Physics in Medicine and Biology*, vol. 61, no. 4, p. 1596, 2016.
- [28] D. Andreuccetti, R. Fossi, and C. Petrucci, "An internet resource for the calculation of the dielectric properties of body tissues in the frequency range 10 Hz - 100 GHz," 1997. [Online]. Available: <http://niremf.ifac.cnr.it/tissprop/>
- [29] P. Gajsek, W. D. Hurt, J. M. Ziriaux, and P. A. Mason, "Parametric dependence of SAR on permittivity values in a man model," *IEEE Transactions on Biomedical Engineering*, vol. 48, no. 10, pp. 1169–1177, 2001.
- [30] I. J. Bahl, S. S. Stuchly, and M. A. Stuchly, "A new microstrip radiator for medical applications," *IEEE Transactions on Microwave Theory and Techniques*, vol. 28, no. 12, pp. 1464–1469, 1980.
- [31] C. Li, Q. Chen, Y. Xie, and T. Wu, "Dosimetric study on eye's exposure to wide band radio frequency electromagnetic fields: variability by the ocular axial length," *Bioelectromagnetics*, vol. 35, no. 5, pp. 324–36, 2014.
- [32] S. B. Rutkove, "Electrical impedance myography: Background, current state, and future directions," *Muscle Nerve*, vol. 40, no. 6, pp. 936–46, 2009.
- [33] R. Pethig and D. B. Kell, "The passive electrical properties of biological systems: their significance in physiology, biophysics and biotechnology," *Physics in Medicine and Biology*, vol. 32, no. 8, p. 933, 1987.
- [34] H. P. Schwan, "Application of UHF impedance measuring techniques in biophysics," *IRE Transactions on Instrumentation*, vol. PGI-4, pp. 75–83, 1955.
- [35] J. L. Schepps and K. R. Foster, "The UHF and microwave dielectric properties of normal and tumour tissues: Variation in dielectric properties with tissue water content," *Physics in Medicine and Biology*, vol. 25, no. 6, pp. 1149–1159, 1980.

- [36] M. T. Jilani, W. P. Wen, M. A. Zakariya, L. Y. Cheong, and M. Z. U. Rehman, "An improved design of microwave biosensor for measurement of tissues moisture," in *2014 IEEE MTT-S International Microwave Workshop Series on RF and Wireless Technologies for Biomedical and Healthcare Applications (IMWS-Bio)*, 2014, Conference Proceedings, pp. 1–3.
- [37] J. Matthie, B. Zarowitz, A. De Lorenzo, A. Andreoli, K. Katzarski, G. Pan, and P. Withers, "Analytic assessment of the various bioimpedance methods used to estimate body water," *Journal of Applied Physiology*, vol. 84, no. 5, pp. 1801–1816, 1998.
- [38] A. Peyman, A. A. Rezazadeh, and C. Gabriel, "Changes in the dielectric properties of rat tissue as a function of age at microwave frequencies," *Physics in Medicine and Biology*, vol. 46, no. 6, pp. 1617–1629, 2001.
- [39] A. Peyman, C. Gabriel, E. H. Grant, G. Vermeeren, and L. Martens, "Variation of the dielectric properties of tissues with age: The effect on the values of SAR in children when exposed to walkie-talkie devices," *Physics in Medicine and Biology*, vol. 54, no. 2, pp. 227–241, 2009.
- [40] W. T. Joines, Y. Zhang, C. Li, and R. L. Jirtle, "The measured electrical properties of normal and malignant human tissues from 50 to 900 MHz," *Medical Physics*, vol. 21, no. 4, pp. 547–550, 1994.
- [41] J. Jossinet and M. Schmitt, "A review of parameters for the bioelectrical characterization of breast tissue," *Annals of the New York Academy of Sciences*, vol. 873, no. 1, pp. 30–41, 1999.
- [42] A. T. Mobashsher, A. Mahmoud, and A. M. Abbosh, "Portable wide-band microwave imaging system for intracranial hemorrhage detection using improved back-projection algorithm with model of effective head permittivity," *Scientific Reports*, vol. 6, p. 20459, 2016.
- [43] *IEEE Recommended Practice for Determining the Peak Spatial-Average Specific Absorption Rate (SAR) in the Human Head from Wireless Communications Devices: Measurement Techniques*, IEEE Standard 1528-2013, 2013.
- [44] *IEEE Standard for Safety Levels with Respect to Human Exposure to Radio Frequency Electromagnetic Fields, 3 kHz to 300 GHz*, IEEE Standard C95.1-2005, 2005.
- [45] T. Wessapan and P. Rattanadecho, "Flow and heat transfer in biological tissue due to electromagnetic near-field exposure effects," *International Journal of Heat and Mass Transfer*, vol. 97, pp. 174–184, 2016.
- [46] M. M. Paulides, J. F. Bakker, M. Linthorst, J. van der Zee, Z. Rijnen, E. Neufeld, P. M. Pattynama, P. P. Jansen, P. C. Levendag, and G. C. van Rhoon, "The clinical feasibility of deep hyperthermia treatment in the head and neck: new challenges for positioning and temperature measurement," *Physics in Medicine and Biology*, vol. 55, no. 9, pp. 2465–80, 2010.
- [47] H. Pftzner, "'Hot nano spots' as an interpretation of so-called non-thermal biological mobile phone effects," *Journal of Electromagnetic Analysis and Applications*, vol. 8, no. 03, p. 62, 2016.
- [48] T. Campi, S. Cruciani, V. D. Santis, and M. Feliziani, "EMF safety and thermal aspects in a pacemaker equipped with a wireless power transfer system working at low frequency," *IEEE Transactions on Microwave Theory and Techniques*, vol. 64, no. 2, pp. 375–382, 2016.
- [49] M. M. Paulides, P. R. Stauffer, E. Neufeld, P. Maccarini, A. Kyriakou, R. A. M. Canters, C. Diederich, J. F. Bakker, and G. C. Van Rhoon, "Simulation techniques in hyperthermia treatment planning," *International Journal of Hyperthermia*, vol. 29, no. 4, pp. 346–357, 2013.
- [50] E. H. Wissler, "Pennes' 1948 paper revisited," *Journal of Applied Physiology*, vol. 85, no. 1, pp. 35–41, 1998.
- [51] *IEEE Recommended Practice for Measurements and Computations of Radio Frequency Electromagnetic Fields With Respect to Human Exposure to Such Fields, 100 kHz to 300 GHz*, IEEE Standard C95.3-2002, 2002.
- [52] Y. Diao, S.-W. Leung, K. H. Chan, W. Sun, Y.-M. Siu, and R. Kong, "The effect of gaze angle on the evaluations of SAR and temperature rise in human eye under plane-wave exposures from 0.9 to 10 GHz," *Radiation Protection Dosimetry*, 2015.
- [53] P. Bernardi, M. Cavagnaro, S. Pisa, and E. Piuzzi, "SAR distribution and temperature increase in an anatomical model of the human eye exposed to the field radiated by the user antenna in a wireless LAN," *IEEE Transactions on Microwave Theory and Techniques*, vol. 46, no. 12, pp. 2074–2082, 1998.
- [54] V. Monebhurrin, C. Dale, J. C. Bolomey, and J. Wiart, "A numerical approach for the determination of the tissue equivalent liquid used during SAR assessments," *IEEE Transactions on Magnetics*, vol. 38, no. 2, pp. 745–748, 2002.
- [55] E. T. McAdams and J. Jossinet, "Tissue impedance: a historical overview," *Physiol Meas*, vol. 16, no. 3 Suppl A, pp. A1–13, 1995.
- [56] S. Kim, J. S. Ho, L. Y. Chen, and A. S. Y. Poon, "Wireless power transfer to a cardiac implant," *Applied Physics Letters*, vol. 101, no. 7, p. 073701, 2012.
- [57] S. Dahdouh, N. Varsier, M. A. N. Ochoa, J. Wiart, A. Peyman, and I. Bloch, "Infants and young children modeling method for numerical dosimetry studies: application to plane wave exposure," *Physics in Medicine and Biology*, vol. 61, no. 4, p. 1500, 2016.
- [58] M. J. Ackerman, "The Visible Human Project," *Proceedings of the IEEE*, vol. 86, no. 3, pp. 504–511, 1998.
- [59] J. Ryckaert, P. De Doncker, R. Meys, A. de Le Hoye, and S. Donnay, "Channel model for wireless communication around human body," *Electronics Letters*, vol. 40, no. 9, pp. 543–544, 2004.
- [60] T. Nagaoka, S. Watanabe, K. Sakurai, E. Kunieda, S. Watanabe, M. Taki, and Y. Yamanaka, "Development of realistic high-resolution whole-body voxel models of Japanese adult males and females of average height and weight, and application of models to radio-frequency electromagnetic-field dosimetry," *Physics in Medicine and Biology*, vol. 49, no. 1, pp. 1–15, 2004.
- [61] A. Christ, W. Kainz, E. G. Hahn, K. Honegger, M. Zefferer, E. Neufeld, W. Rascher, R. Janka, W. Bautz, J. Chen, B. Kiefer, P. Schmitt, H. P. Hollenbach, J. Shen, M. Oberle, D. Szczerba, A. Kam, J. W. Guag, and N. Kuster, "The Virtual Family—development of surface-based anatomical models of two adults and two children for dosimetric simulations," *Physics in Medicine and Biology*, vol. 55, no. 2, pp. N23–38, 2010.
- [62] A. F. Abdelaziz, Q. H. Abbasi, K. Yang, K. Qaraqe, Y. Hao, and A. Alomainy, "Terahertz signal propagation analysis inside the human skin," in *2015 IEEE 11th International Conference on Wireless and Mobile Computing, Networking and Communications (WiMob)*, 2015, Conference Proceedings, pp. 15–19.
- [63] G. R. G. Raju, "Dielectric constant of binary mixtures of liquids," in *Conference on Electrical Insulation and Dielectric Phenomena 1988. Annual Report.*, 1988, Conference Proceedings, pp. 357–363.
- [64] S. Allen, G. Kantor, H. Bassen, and P. Ruggera, "Quality-assurance reports: CDRH RF phantom for hyperthermia systems evaluations," *International Journal of Hyperthermia*, vol. 4, no. 1, pp. 17–23, 1988.
- [65] A. W. Guy, "Analyses of electromagnetic fields induced in biological tissues by thermographic studies on equivalent phantom models," *IEEE Transactions on Microwave Theory and Techniques*, vol. 16, no. 2, pp. 205–214, 1971.
- [66] C.-K. Chou, G.-W. Chen, A. W. Guy, and K. H. Luk, "Formulas for preparing phantom muscle tissue at various radiofrequencies," *Bioelectromagnetics*, vol. 5, no. 4, pp. 435–441, 1984.
- [67] B. Kibret, A. K. Teshome, and D. T. H. Lai, "Analysis of the human body as an antenna for wireless implant communication," *IEEE Transactions on Antennas and Propagation*, vol. 64, no. 4, pp. 1466–1476, 2016.
- [68] J. B. Ferreira, A. A. de Salles, and R. C. E. Fernández, "SAR simulations of EMF exposure due to tablet operation close to the user's body," in *2015 SBMO/IEEE MTT-S International Microwave and Optoelectronics Conference (IMOC)*, 2015, Conference Proceedings, pp. 1–5.